fermentation

MDPI

Article

Insights into Proteomics Reveal Mechanisms of Ethanol-Enhanced Bacterial Cellulose Biosynthesis by *Komagataeibacter nataicola*

Shuangwen Fei [1,†], Xuan Yang [1,2,3,†], Wentao Xu [3], Jiachao Zhang [1,4], Jun Li [1], Huamei Chen [1], Xue Lin [1], Sixin Liu [4,5,6,*] and Congfa Li [1,4,5,*]

[1] School of Food Science and Engineering, Hainan University, Haikou 570228, China; swen.f@hainanu.edu.cn (S.F.)
[2] College of Biosystems Engineering and Food Science, Key Laboratory for Agro-Products Nutritional Evaluation of Ministry of Agriculture and Rural Affairs, Interdisciplinary Research Center on Optical Agricultural and Food Engineering, Zhejiang University, No. 866 Yuhangtang Road, Hangzhou 310058, China
[3] College of Food Science and Nutritional Engineering, China Agricultural University, Beijing 100083, China
[4] Key Laboratory of Tropical Agricultural Products Processing Technology of Haikou City, Haikou 570228, China
[5] Key Laboratory of Food Nutrition and Functional Food of Hainan Province, Haikou 570228, China
[6] School of Science, Hainan University, Haikou 570228, China
* Correspondence: sixinliu@hainanu.edu.cn (S.L.); congfa@hainanu.edu.cn (C.L.); Tel./Fax: +86-898-66213379 (S.L.)
† These authors contributed equally to this work.

Abstract: Nata de coco, known as bacterial cellulose (BC), has been given much attention in the food industry and biomaterial areas due to its specific properties such as low calorie content, high content of fiber, high purity and high biocompatibility. *Komagataeibacter* spp. are indispensable microorganisms for BC production due to their highly efficient production. Here, proteomics was applied to investigate the metabolism regulation mechanisms of BC yield improvements in *K. nataicola* Y19 by 48 ± 3% after ethanol supplementation. The results evidenced that differentially expressed proteins involved in the BC biosynthesis system, glycolytic pathway, TCA cycle and oxidative phosphorylation process were up-regulated. The proteins accelerated the BC biosynthesis by providing more energy and via intermediate metabolites. Furthermore, the elongation factor Tu, chaperone DnaK and translocase subunit SecB may be involved in the BC synthesis procedure by regulating electron transfer, hydrolysis of ATP and protein transformation. Moreover, the ethanol-enhanced BC biosynthesis may be associated with the decreased expression of endoglucanase. This research elucidates the proteomics mechanism of higher BC production based on ethanol addition, providing references for nata de coco production efficiency and the synthetic regulation of bacterial cellulose in the future.

Keywords: nata de coco; bacterial cellulose; biosynthesis regulation; *Komagataeibacter nataicola*; proteomics

Citation: Fei, S.; Yang, X.; Xu, W.; Zhang, J.; Li, J.; Chen, H.; Lin, X.; Liu, S.; Li, C. Insights into Proteomics Reveal Mechanisms of Ethanol-Enhanced Bacterial Cellulose Biosynthesis by *Komagataeibacter nataicola*. *Fermentation* **2023**, *9*, 575. https://doi.org/10.3390/fermentation9060575

Academic Editor: Yuanda Song

Received: 17 May 2023
Revised: 6 June 2023
Accepted: 13 June 2023
Published: 17 June 2023

1. Introduction

Nata de coco is a traditional dessert which has been firstly fermented in waste coconut water in southeast Asian countries such as Philippines, Indonesia and Vietnam. Nata de coco has gained extensive popularity owing not only as a weight-loss food with good elastic taste, low caloric and high fiber contents [1], but also its excellent material properties in the field of biomaterials [2]. In fact, nata de coco is a gelatinous microbial extracellular polysaccharide consisting of linear β-1,4-D-glucose units, widely known as bacterial cellulose (BC). The isolation and purification of the BC product do not require complicated processes and harsh chemical treatments, because it has a higher purity than plant cellulose.

On the other hand, the high water-holding capability and uniformed porosity of BC make it a remarkable material for physical interaction with active compounds. Thus, BC can be used as a biodegradable film [3] and food-modified dietary fiber [4]. In particular, probiotic lactic acid bacteria can be immobilized in BC against digestion by gastric juices and bile salt solution, providing the possibility for biotechnological applications for the immobilization of other microorganisms [5]. These BC-based materials can be widely used in daily life and the food industry [6].

However, the lack of efficient and stable fermentation systems is still a challenge for the large-scale commercial low-cost production of nata de coco, as well as BC. Over the past decades, strategies to improve nata de coco or BC yield have aroused worldwide attentions. Generally, culture method improvement, culture medium optimization, the identification of new microorganism strains and genetic engineering have been applied to improve nata de coco or BC yield [7]. Among them, the addition of inducers can be a convenient and effective way to improve BC yield. Researchers have especially reported that ethanol has a strong promoting effect on BC yield [8–10]. The mechanism of ethanol supplementation contributing to a higher BC yield has been explored preliminarily using a different strategy during the past decades. Adenosine triphosphate (ATP) is essential for the final intracellular BC secretion, providing sufficient energy for the whole process of BC synthesis [11,12]. It was reported that ethanol resulted in higher ATP levels with the help of spectrophotometry in the case of the *Komagataeibacter xylinum* during BC synthesis [13]. Moreover, Yunoki et al. used ^{13}C-labeled carbon to investigate the role of ethanol in the improvement of BC production and found that the Entner–Doudoroff pathway was repressed in the presence of ethanol [14]. BC biosynthesis is closely linked to the metabolic processes of glucose [11], which determine the efficiency of BC synthesis, as well as the direction of carbon metabolic flow. Studies on *Acetobacter* sp. grown on a culture medium containing ethanol concluded that the activity of glucokinase and fructokinase were induced, while glucose-6-phosphate dehydrogenase and gluconokinase were inhibited, thereby making more glucose flow into UDP-glucose, the precursor of BC, and limiting glucose from flowing into the hexose monophosphate (HMP) pathway [10,13]. To better understand the systemic cellular response of *K. xylinus* in the presence of ethanol, transcriptomes have been performed in Ryngajłło's study [9], in which ethanol had a positive effect on protein synthesis and electron-accepting reactions, while having an inhibitory effect on the TCA cycle, glycolysis/gluconeogenesis, electron-donating reactions, protein degradation and stress response. In another study, time-dependent transcriptome technology was used to explore the effect of ethanol on *Acetobacter aceti* NBRC 14818, and the results showed that ethanol could act as an alternative energy source partially oxidized into acetic acid in the periplasm by alcohol dehydrogenase (ADH) and aldehyde dehydrogenase (ALDH), providing extra metabolites for the tricarboxylic acid (TCA) cycle [15].

Komagataeibacter, formerly known as *Acetobacter* or *Gluconacetobacter*, is an excellent and typical genus to produce BC and nata de coco, which has been widely used because of its highly efficient production [4]. Its cellulose biosynthesis pathway mainly consists of phosphoglucomutase, UDP-glucose pyrophosphorylase and bacterial cellulose synthase (BCS) [7]. Phosphoglucomutase catalyzes glucose-6-phosphate into glucose-1-phosphate, which is subsequently transformed into UDP-glucose through the catalysis of UDP-glucose pyrophosphorylase. BCS is composed of four subunits (BcsA, BcsB, BcsC and BcsD), which are responsible for the assembly and expulsion of cellulose chains [12,16]. Previous research showed that the genes of *K. xylinus* E25 encoding the bcsABCD operon were induced in the presence of ethanol, which may result in a higher BC yield [15].

Over the past decade, genetically engineered *Komagataeibacter* strains via synthetic biology have received extensive attention. Researchers have tried to improve the BC yield through *Komagataeibacter* strains, and produced new functionalities in BC through synthetic biology [17]. Chien et al. [18] and Liu et al. [19] transformed *Vitreoscilla* hemoglobin (VHb)-encoding gene *vgb* into *A. xylinum* and *Gluconacetobacter xylinus*, respectively, which could promote the BC production by increasing oxygen tensions. In the aforementioned research,

however, BC yield was only increased two times, which dissatisfies the huge needs of factories and the market. Therefore, it is necessary to screen superior strains with a higher production efficiency and conduct more in-depth research that significantly improves BC yield.

Proteomics has been widely used as a tool to comprehensively understand the biological response of microorganisms under external treatment [20]. Recently, metaproteomic characteristics of *Komagataeibacter* involved in the acetification process and high-acid spirit vinegar production were investigated [21,22]. The expression of the proteins related to the amino acid metabolism, protein biosynthesis and energy production in *Komagataeibacter europaeus* was up-regulated in the cycle-loading phase to defend against the high level of acid [22]. The expression of proteins related to stress responses and the TCA cycle was up-regulated, strengthening the ability of *Komagataeibacter* spp. to resist the high-acid environment [21]. However, proteomics of the genus *Komagataeibacter* relating BC synthesis has not been reported, and the effect of ethanol supplementation on the protein profile and regulatory mechanism remains unclear. In our previous research, the yield of nata de coco was improved eight times after ethanol addition (Supplement Figure S1). In order to investigate its mechanism and exclude the interference of coconut water components, a HS medium with ethanol supplement was used in this research. Proteomics was conducted to explore the changes in the protein spectrum of *K. nataicola* Y19 after ethanol addition, which helped us better understand the metabolic pathways and the key influencing factors of high BC production. Meanwhile, *RT-qPCR* was applied to validate our proteomics results. The comprehensive description of the protein profile could facilitate the understanding of the protein mechanism and key node of high BC yield of *K. nataicola* Y19, providing theoretical basis for cellulose synthetics biology in research, along with the yield improvement of nata de coco in the industry.

2. Materials and Methods

2.1. Strains, Media and Inoculum Preparation

The strain *K. nataicola* Y19 was isolated from a BC fermentation factory (Haikou, China) and stored at the School of Food Science and Engineering, Hainan University. The Hestrin–Schramm medium (HS) was used as the basal medium, which consists of 20 g/L glucose, 5 g/L peptones, 5 g/L yeast extract, 2.7 g/L Na_2HPO_4 and 1.15 g/L citric acid, with the initial pH adjusted to 5.0 before sterilization at 121 °C for 20 min. The primary inoculum was prepared by transferring the culture from a slant to a flask containing broth, which was then incubated at 30 °C for 2 d without agitation.

2.2. Cellulose Fermentation and Viable Cell Number Determination

Previously, we found that 1% (*v*/*v*) ethanol and 1% (*v*/*v*) acetic acid had the most significantly positive effect on BC yield improvement of *K. nataicola* Y19. As a consequence, 1% (*v*/*v*) ethanol and 1% (*v*/*v*) acetic acid were chosen as the experimental concentrations in this section. The 2% (*v*/*v*) primary inoculum was added to 500 mL flasks containing 100 mL HS medium with 1% (*v*/*v*) ethanol and 1% (*v*/*v*) acetic acid, respectively, and then cultivated at 30 °C for 7 d. Fermentation in the HS medium was set as the control. The harvested BC membrane was purified by distilled water and then treated with 0.5 M NaOH at 90 °C for 24 h. After that, BC was washed with distilled water to eliminate embedded cell debris and impurities. The BC yield was obtained according to Ryngajłło's research [9], with appropriate modifications. The purified BC membranes were subsequently dried at 105 °C until they achieved a constant weight, before being weighed. The viable cell number was determined using the plate dilution method [23]. First, the broth containing the BC membrane was treated with cellulase (10 kU/g Jinggang ShangTian, Japan) at 37 °C for 3 h to hydrolyze cellulose. Then, the free cell number was determined by counting the colony-forming units. The bacterial suspension containing bacteria was serially diluted with 0.9% saline, and then 100 µL of the bacterial suspension from each serially diluted solution was spread on HS plates. The plates were then incubated at 30 °C, and the colonies formed were

counted within 3–4 days. Each bacteria suspension was performed in triplicate. A scanning electron microscope (SEM, Phenom-World BV, Eindhoven, The Netherlands) was used to observe the BC micromorphologies of the experimental group and the control. Before detection, the BC membrane was immersed in liquid nitrogen to maintain the stability of the structure. Then, it was quenched from the middle of the BC membrane, and the quenched sample was taken for vacuum freeze-drying at −80 °C.

2.3. Extraction of Intracellular Proteins

According to the results presented in Section 2.2, ethanol showed a better promoting effect on BC yield; thus, Y19 in the basal medium with additional ethanol was chosen for subsequent experiments. At the end of fermentation, the intracellular proteins of Y19 trapped in the BC membrane were extracted for proteomics measurements. After harvesting, the BC membrane was lyophilized (Labconco, Kansas City, MO, USA). After that, 1.2 g of the freeze-dried BC membrane from each group was ground in a mortar with liquid nitrogen, and then resuspended in a lysis buffer containing 7 M urea (Amresco, Solon, OH, USA), 2 M thiourea (Sigma, Saint Louis, MO, USA), 4% (*w*/*v*) CHAPS (Sigma, USA), 1% (*w*/*v*) DTT (Sigma, Saint Louis, MO, USA), 1% (*v*/*v*) pH 4–7 IPG buffer (GE Healthcare, USA) and 0.5% (*v*/*v*) protease inhibitor cocktail (GE Healthcare, Little Chalfont, PA, USA), before being sonicated intermittently using an ultrasonic instrument (KQ-500DE, Shumei Kunshan Co., Kunshan, China) for 99 s with a nominal power of 300 W. Subsequently, the ultrasound-treated solution was centrifuged at 15,000× *g* for 20 min at 4 °C to remove non-lysed cells and cell debris. The proteins in the BC membrane were desalted and purified using a 2D Clean-up Kit (GE Healthcare, Piscataway, NJ, USA), according to the manufacturer's instructions. The protein concentrations were determined through the Coomassie Brilliant Blue staining analyses. Finally, the protein samples were air-dried at room temperature and then stored at −80 °C until further use. All samples were prepared in triplicate.

2.4. Two-Dimensional Electrophoresis and Data Analysis

The obtained intracellular proteins of Y19 in each group were separated via two-dimensional electrophoresis, according to Cheng's study [24]. Isoelectric focusing (IEF) was performed in IPG strips (pH 4–7, 13 cm, GE Healthcare, Piscataway, NJ, USA) on a Multiphor III system (GE Healthcare, Piscataway, NJ, USA). IPG strips were rehydrated by 250 µL of a rehydration buffer containing 550 µg proteins, 7 M urea, 2 M thiourea, 2% (*w*/*v*) CHAPS, 65 mM DTT, 2% (*v*/*v*) IPG buffer (pH 4–7, GE Healthcare, Piscataway, NJ, USA) and 0.002% (*v*/*v*) bromophenol blue (Beyotime, Shanghai, China). Subsequently, the IPG strips were rehydrated again in 4 mL of immobilized DryStrip cover fluid (Cytiva, Marlborough, MA, USA) at 25 °C for 14 h. The running conditions were as follows: 500 V for 500 Vh, followed by 1000–8000 V for 19,800 Vh, and finally 500 V for 10 h, at 20 °C, 50 µA. For the reduction and alkylation of proteins, the treated IPG strips were equilibrated with an equilibration buffer (150 mM Tris-HCl, 8 M urea, 20% (*v*/*v*) glycerol, 2% (*w*/*v*) SDS and 100 mM DTT). Then, the IPG strips were equilibrated again with the same buffer after replacing the DTT with 250 mM iodoacetamide (Sigma, Saint Louis, MO, USA). After the reduction and alkylation processes, the strips were loaded onto a slab gel (20 cm × 20 cm × 1 mm) for sodium dodecyl sulfate polyacrylamide gel electrophoresis (SDS-PAGE). The electrophoresis was performed in 4% stacking gel and 12.5% separating gels. The IPG strip gel was enclosed with 0.5% low-melting agarose gels. The SDS-PAGE running buffer contained 3% (*w*/*v*) Tris, 1.4% (*w*/*v*) glycine and 0.1% (*w*/*v*) SDS. The 4% stacking gels and 12.5% separating gels were used with a constant current of 20 mA (600 V, 40 min) and 40 mA (600 V, 5 h), respectively. Finally, the proteins were visualized on gels by Coomassie Brilliant Blue R-250 (Amresco, Solon, OH, USA).

Image digitization was performed with an Image Scanner (GE Healthcare, Piscataway, NJ, USA), and the protein expression levels in the 2D gel images were compared by using the Image Master 2D Platinum version 7.0 software (GE Healthcare, Piscataway, NJ, USA).

To account for experimental variation, at least three gels with protein extracts obtained from independent experiments were analyzed using Image Master 2D Platinum version 7.0 software (GE Healthcare, Piscataway, NJ, USA). The normalized intensity of the spots on three replicate 2D gels was averaged, and the standard deviation was calculated. A one-way ANOVA ($p < 0.05$) was used to determine the statistical significance of the difference in spot intensities between the control and experimental groups. The ratios of the two groups were calculated based on the differences in standardized abundance.

2.5. Protein Identification and Database Searching

Protein spots were manually excised from the 2D gels, destained using 25 mM NH_4HCO_3 in 40% (v/v) acetonitrile and dried in a aSpeed Vac Concentrator for 5 min. Subsequently, the protein was digested by 0.01 μg/μL trypsin in 30 μL of 25 mM NH_4HCO_3 at 37 °C for 12 h, followed by an addition of 1 mL of 2% (v/v) trifluoroacetic acid to terminate the hydrolysis and centrifuging at 1500× g for 5 min at 4 °C (Allegra 64R Centrifuge, Beckman Coulter, California, Germany), to collect and dry the supernatant. The tryptic peptides in the supernatant were extracted with 10 μL of a solution containing 0.1% (v/v) trifluoroacetic acid and 50% (v/v) acetonitrile. MALDI-TOF/TOF-MS experiments were performed according to Sun's research [25]. Of the tryptic peptides, 1 μL was mixed with MALDI matrix (5 mg/mL (α-cyano-4-hydroxycinnamic acid (CHCA) and 0.1% trifluoroacetic acid (TFA) and 50% acetonitrile, and then spotted onto the MALDI target plates for analysis using an ABI 4800 MALDI-TOF/TOF mass spectrometer (Applied Biosystems, Foster City, CA, USA). MS spectra were gathered with 1600 laser shots per spectrum and the MS/MS spectra were acquired with 2500 laser shots per fragmentation spectrum. The top 10 strongest peaks from each MS spectra were selected as precursor ions for the acquisition of the MS/MS fragmentation spectra. The identification of peptide and protein was performed using the GPS Explorer software (version 3.6, Applied Biosystems, Foster City, CA, USA) paired with the MASCOT search program (Matrix Science, http://www.matrixscience.com/ (accessed on 25 May 2022.)). The NCBI (National Center for Biotechnology Information) database was used as a search database, the *Komagataeibacter* database was used as the species query database and the restriction enzyme cutting site was trypsin. Carboxymethylation and oxidation were selected as variable modifications. One missed cleavage was allowed. The precursor error tolerance was set to 0.2 Da, and the MS/MS fragment error tolerance was set to 0.3 Da. All identified proteins had scores > 61 and individual ion scores > 21, with p-values < 0.05. All MS/MS spectra were further validated manually. The functional cluster analysis of significantly differentially expressed proteins was performed based on the biological process in the Uniport database (http://www.uniprot.org/ (accessed on 9 June 2022)).

2.6. RNA Extraction and cDNA Synthesis

To further confirm the proteomics results of *K. nataicola* in the presence of ethanol, the transcription levels of four key genes encoding the enzymes involved in cellulose synthesis, HMP pathway and oxidative phosphorylation were detected. RNA extraction and cDNA synthesis were performed according to the method proposed in Galisa's study [26], with some modifications. RNA was isolated with Trizol (Tiangen, Beijing, China), according to the manufacturer's protocol. The quality of the RNA was confirmed using 2% agarose gel electrophoresis. First-strand cDNA synthesis was carried out by using the FastQuant cDNA Reverse Kit (Tiangen, Beijing, China), according to the manufacturer's protocol. Reverse transcription reactions were carried out with 3 μg of total RNA and 2 μg of FQ-RT Primer Mix, according to the manufacturer's protocol. The cDNA was diluted at a ratio of 1:5 and then used in the RT-qPCR reaction.

2.7. RT-qPCR

RT-qPCR experiments were performed in triplicate by using the Real Master PCR Mix kit (SYBR Green) (Tiangen, Beijing, China) in the CFX 96 Real-Time System (Bio-Rad,

Hercules, CA, USA). The volume of each sample was set to 25 µL. The thermal cycling program was set as follows: 50 °C for 10 min and 95 °C for 5 min; followed by 40 cycles at 95 °C for 30 s, 58 °C for 30 s (optimized for each primer pair), and 72 °C for 60 s; a melting curve stage at 95 °C for 15 s; 60 °C for 1 min; 95 °C for 30 s; and 60 °C for 15 s. Reactions with non-specific fluorescence were excluded three times. Gene-specific primers (Table 1) were designed for each target gene. Samples from the three biological replicates were assayed in triplicate. The expression levels were normalized according to those of *G. europaeus* 16S rRNA [27]. The $2^{-\Delta\Delta CT}$ method was used to calculate the relative levels of gene expression [28].

Table 1. Primer sequences used in RT-qPCR.

Gene Name	Forward Primer	Reverse Primer	PCR Size (bp)
K. nataicola 16S rRNA	5′ GTGCTACAATGGCGGTGACA 3′	5′ TGACGGGCGGTGTGTACAAG 3′	137
Phosphoglucomutase (*pgm*)	5′ CAGATCCGCATGGACTGTTCT 3′	5′ GGTCCGCATCGGTATCATTG 3′	100
Phosphoglycerate kinase (*pgk*)	5′ CGCGCTGACCTGAATGTTC 3′	5′ ATCACCTTCGCACCCTTCTG 3′	110
Phosphopyruvate hydratase (*eno*)	5′ CCGATCGACATTCAGGAATTC 3′	5′ CCCGAGAGGCTTTTTTTAAGC 3′	110
Ppa inorganic pyrophosphatase (*ppa*)	5′ GACAAGGTGCACCCGTACTATTC 3′	5′ GCCCTTCTCCAGGTCCTTGTA 3′	111

3. Results

3.1. Effects of Ethanol and Acetic Acid on BC Yield and Structure

The BC yield and viable cells of Y19 were detected after static culture in the HS medium for 7 d, with the addition of ethanol and acetic acid, respectively. As shown in Figure 1, the addition of ethanol resulted in a 48 ± 3% increase in BC yield, and the addition of acetic acid resulted in a 19 ± 2% increase in BC yield compared with the control group. The bacterial biomass of Y19 reached the mid-stationary phase after culturing in the control medium for 3 d, while it reached the mid-stationary phase in the ethanol and acetic acid group at 4 d and 5 d, respectively. However, there was no significant difference among these groups. The BC membrane structure in the three groups was commonly characterized by porous morphology and an interconnected network, which was consistent with the typical morphology of a BC membrane (Supplement Figure S2). The cellulose fibrils in the control were thicker and the pores were larger and distributed more dispersedly. On the contrary, cellulose fibrils in the ethanol group were slenderer and the distribution of pores between the fibrils was denser. The network of the BC membrane in the acetic acid group was unevenly distributed as a radial pattern.

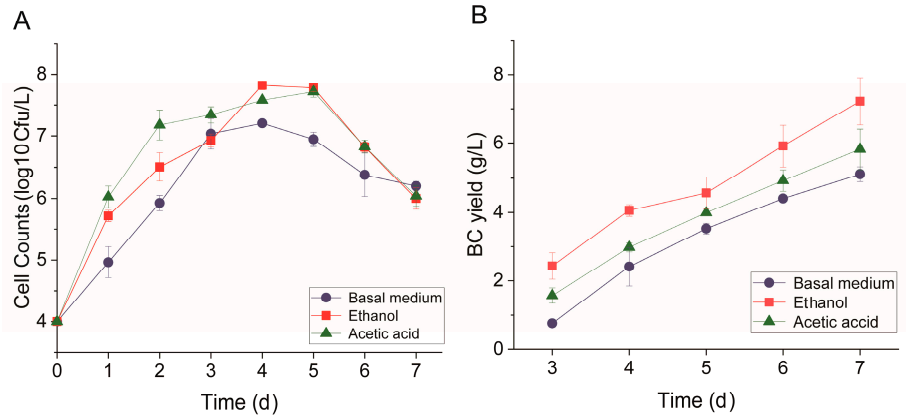

Figure 1. Time course of *K. nataicola* Y19 growth (**A**) and BC yield (**B**) in the basal medium (blue rhombus), the basal medium with ethanol (red square) and acetic acid (green triangle).

3.2. Proteomics Analysis of K. nataicola during Ethanol-Enhanced Fermentation

Proteomics research of Y19 was performed after ethanol treatment. Proteomics profiling analysis identified several novel proteins associated with BC biosynthesis, including

natively secreted proteins and intracellular proteins. The representative 2D images of the Y19 protein profiles of the control and the ethanol-enhanced group are shown in Figure 2. Proteins with an isoelectric point between pH 4 and 7 and a molecular weight between 10 and 120 kDa were separated, and 847 gel spots were matched across three independent experiments (Supplement Figure S3). Finally, 38 protein spots were differentially expressed in the ethanol group under the standards of ratio > 1.5 and p-value < 0.05. Of these 38 spots, 28 proteins were successfully identified, including 19 with an up-regulated expression and 9 with a down-regulated expression, as summarized in Table 2. After the addition of ethanol, the expression of endoglucanase was decreased by 4.05%, while the expressions of succinyl-CoA synthetase subunit alpha, aconitate hydratase, succinate dehydrogenase iron-sulfur subunit and 3-oxoacyl-ACP synthase in the TCA cycle were increased by 1.92%, 2.23%, 2.31% and 1.68%, respectively (Figure 3). Furthermore, FoF1-ATP synthase subunits (α, β and γ), which are closely related to ATP synthesis, were increased by more than 2.18%. In particular, the elongation factor Tu and translocase subunit SecB were clearly increased by 7.01% and 5.13%, respectively. The biological functions of these proteins were analyzed via clustering analysis, shown in Figure 4. The majority of the differentially expressed proteins were involved in ATP binding, tricarboxylic acid cycle, ATP transport, glycolysis, protein biosynthesis and protein folding. These results indicated that the glucose metabolism and energy cycle were more active after the addition of ethanol.

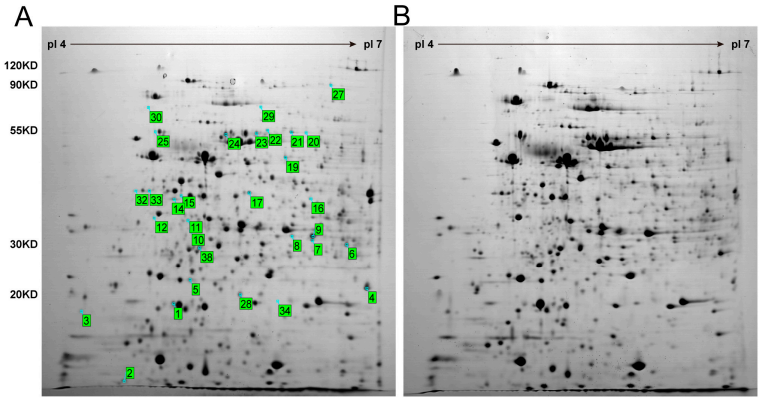

Figure 2. Representative 2D gel profiles of total proteins from *K. nataicola* Y19 in the basal medium with ethanol (**A**) and the basal medium. (**B**) The numbered spots are significantly differentially expressed proteins in *K. nataicola* Y19 in the presence of ethanol (Range ratio > 1.5, $p < 0.05$).

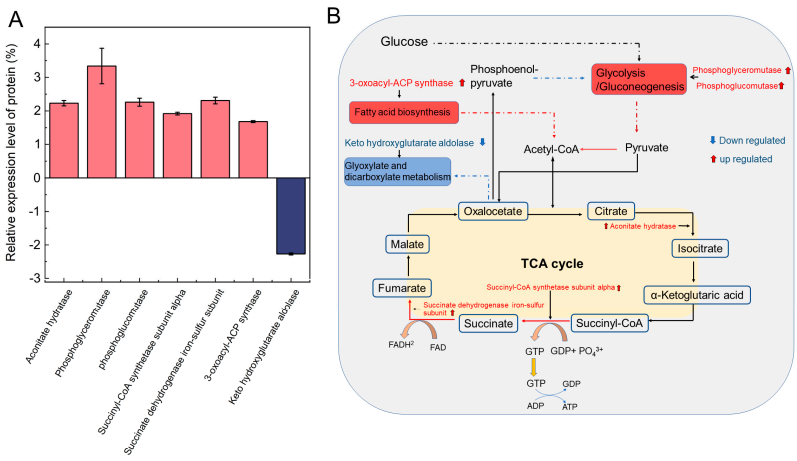

Figure 3. Significantly differentially expressed proteins involved in the TCA cycle in *K. nataicola* Y19 in the presence of ethanol. (**A**) Relative expression level of significantly differentially expressed proteins. (**B**) The distribution of differentially expressed proteins in the TCA cycle. Red: up-regulated proteins; blue: down-regulated proteins.

Table 2. Identification of differentially expressed proteins in *K. nataicola* Y19 after the addition of ethanol to the fermentation medium.

Protein Name	Spot	NCBI Accession No. (gi)	Relative Change Ratio	*p*-Value	Protein PI Exp./Theor.	Protein MW Exp./Theor.	Protein Score	Total Ion Score
Bacterioferritin	1	gi|517915025	−3.56973	3.05×10^{-3}	5.17/5.17	23,103.6/23,118.12	291	259
Short-chain dehydrogenase	2	gi|498194358	2.04802	6.09×10^{-4}	5.22/5.22	30,091.2/30,109.84	153	170
Preprotein translocase subunit SecB	3	gi|503872550	5.13468	1.97×10^{-2}	4.43/4.42	21,359/21,372.33	285	246
Keto hydroxyglutarate aldolase	4	gi|498193026	−2.26968	4.03×10^{-3}	5.76/5.75	20,515.9/20,528.93	210	182
ATP-dependent Clp protease ClpP	5	gi|498193945	−1.70585	4.69×10^{-5}	5.46/5.46	25,122.7/25,138.50	322	254
Putative 2-keto-4-pentenoate hydratase-like protein	6	gi|295977509	−4.69407	3.11×10^{-2}	5.78/5.78	27,325/27,341.80	67	59
Succinyl-CoA synthetase subunit alpha	7	gi|498195575	1.92323	4.79×10^{-4}	5.74/5.74	29,491.2/29,509.89	160	125
Dihydrofolate reductase	8 9	gi|498197255	0.718128658	4.08×10^{-3}/ 5.33×10^{-3}	6.08/6.08	32,787.5/32,808.01	155 & 255 & 242	143 & 236 & 222
Endopeptidase	10	gi|494639202	2.20294	$2.73 \times 10-3$	6.01/6.01	52,500.3/52,532.33	89	78
Tryptophan synthase subunit alpha	11	gi|517915408	2.31726	6.41×10^{-4}	4.97/4.97	29,003.1/29,021.18	171	140
Elongation factor Tu	12/ 32/ 33	gi|494641674	2.20755/ 2.81953/ 2.00149	1.23×10^{-3}/ 1.00×10^{-5}/ 2.78×10^{-3}	5.21/5.21	43,038/43,065.11	381 & 335 & 384	302 & 242 & 304
Endoglucanase	14	gi|517916528	−4.50838	8.01×10^{-5}	5.69/5.69	35,858.8/35,881.21	112	96
GTP-binding protein TypA	15	gi|498201343	4.97347	2.17×10^{-4}	5.34/5.34	67,064.9/ 67,106.43	260	196
FoF1-ATP synthase subunit gamma	16	gi|498194795	2.28583	2.54×10^{-3}	9.32/9.32	31,908.6/31,928.59	189	194
Hypothetical protein	17	gi|498198670	−2.34605	5.71×10^{-3}	5.48/5.48	30,753.7/30,772.93	91	78
3-oxoacyl-ACP synthase	19	gi|503870050	1.68533	2.24×10^{-3}	5.67/5.67	44,656.5/44,684.51	318	246
Phosphoglucomutase	21	gi|498197944	2.26054/	4.93×10^{-4}	5.67/5.67	59,569.2/59,606.28	268	187
Phosphoglyceromutase	23	gi|517914319	3.33922	2.47×10^{-3}	5.67/5.67	55,241/55,275.56	287	258
FoF1-ATP synthase subunit alpha	24	gi|498194792	2.18281	1.67×10^{-3}	5.5/5.50	55,345.9/55,380.43	614	457
FoF1-ATP synthase subunit beta	25	gi|517921194	3.17124	5.57×10^{-3}	4.92/4.92	49,902.8/49,933.85	638	501
Aconitate hydratase	27	gi|517914984	2.23475	3.57×10^{-4}	6.09/6.09	96,468.8/96,529.47	606	408
Carbohydrate kinase	28	gi|517916350	−3.89058	5.36×10^{-4}	5.28/5.28	18,122.8/18,134.81	118	97
Molecular chaperone DnaK	30	gi|498194452	4.11107	6.14×10^{-3}	4.89/4.89	67,553/67,594.39	297	230
Adenylate kinase	34	gi|498192553	9.06655	1.17×10^{-2}	7.59/7.59	24,247.5/24,262.91	204	184
Succinate dehydrogenase iron-sulfur subunit	38	gi|498195041	2.31759	1.74×10^{-3}	5.37/5.37	29,203.6/29,222.53	151	115

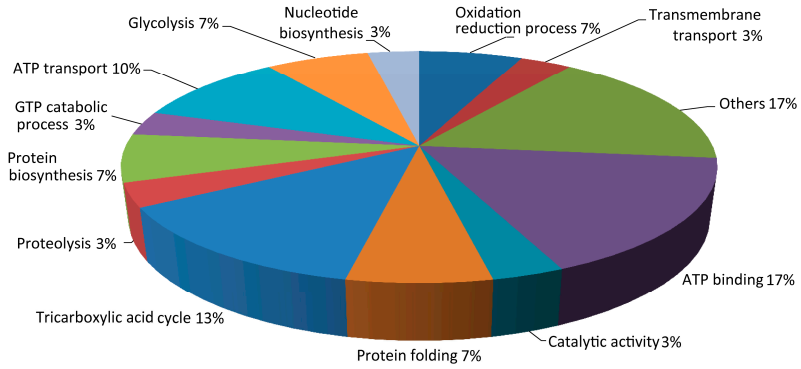

Figure 4. The biological process of significantly differentially expressed proteins of *K. nataicola* Y19 in the presence of ethanol.

3.3. Regulation of Gene Expression in BC Synthesis

To further investigate the effect of ethanol on the carbon metabolic pathway of *K. nataicola* Y19, the transcription levels of representative genes, including phosphoglucomutase (*pgm*), phosphoglycerate kinase (*pgk*), phosphopyruvate hydratase (*eno*) and inorganic pyrophosphatase (*ppa*), were determined. As shown in Figure 5, the expression of *pgm* was up-regulated 4.87-fold, while the expression of *Eno* gene was down-regulated 0.75-fold after ethanol addition. The expression of *pgk* in the presence of ethanol was increased slightly ($p < 0.05$). The transcription of *ppa* involved in oxidative phosphorylation was increased 3.97-fold.

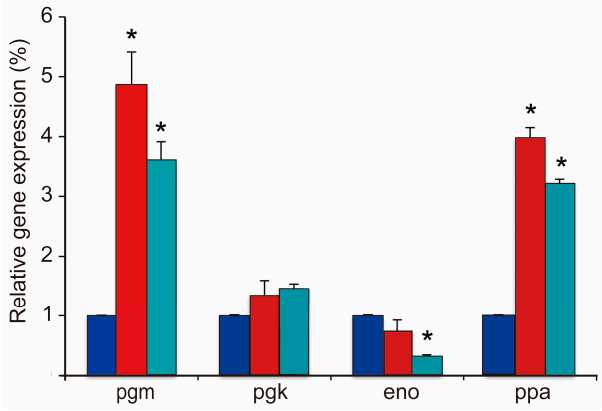

Figure 5. Gene expression of the rate-limiting enzyme in cellulose synthesis, HMP pathway and oxidative phosphorylation. Blue: basal medium; red: basal medium with ethanol; cyan: acetic acid; "*": $p < 0.05$. *pgm:* phosphoglucomutase; *pgk*: phosphoglycerate kinase; *eno*: phosphopyruvate hydratase; *ppa*: inorganic pyrophosphatase.

4. Discussion

Ethanol has been used as a low-cost additive in BC production because it can significantly promote BC yield [29]. Several studies have revealed its molecular mechanism at the metabolite and protein levels by detecting the content of the key metabolites and enzyme activity in BC synthesis, TCA cycle, glycolysis and the HMP pathway [13,14,30]. Recently, the gene expression profile of *K. xylinus* was carried out in Ryngajłło's research [9] to investigate the effect of ethanol on its systemic cellular response. However, the effect of ethanol on the proteomics of the *Komagataeibacter* spp. during BC synthesis has not been reported. The genome and transcriptome reveal genetic code and gene expression, while microorganism activities are mainly completed by the proteome. Therefore, proteomics could be an accurate and clearer method to demonstrate the metabolic regulation of *Komagataeibacter* under the stimulation of ethanol. In this work, 1% (*v*/*v*) ethanol addition resulted in a higher BC yield (48 ± 3%) (Figure 1), and the total proteins of *K. nataicola* Y19

in the basal medium containing ethanol were compared with that in the basal medium without ethanol.

Our results show that ethanol could up-regulate the expression of phosphoglucomutase at both proteomics and transcription levels (Table 2 and Figure 5), which is in accordance with previous observations [9]. Phosphoglucomutase, a key enzyme closely related to BC synthesis [31], catalyzes the conversion of glucose-6-phosphate into glucose-1-phosphate, which is a very important step in BC synthesis [32]. These results imply that the route leading to cellulose formation was induced and the glucose flux toward glycolysis and the HMP pathway was down-regulated in the presence of ethanol, which is consistent with the results of key enzyme activities in other research [33]. Glycolysis is an oxygen-independent metabolic pathway that regulates the initial stages of glucose absorption in bacteria. Phosphoglyceromutase and phosphoglycerate kinase are involved in the first ATP-generating step and the penultimate step of glycolysis, respectively. Other results from this research showed that the transcriptional levels of phosphoglyceromutase and phosphoglycerate kinase, as well as their content in *K. nataicola* Y19, were up-regulated, while the transcriptional level of phosphopyruvate hydratase was down-regulated, which may lead to the accumulation of 2-phosphoglycerate. Therefore, it can be concluded that ethanol can reduce glucose flux toward glycolysis and the TCA cycle, providing more precursors for BC synthesis [30].

It has been postulated that an increased cellulose yield is closely linked to the TCA cycle and ATP levels [9,13]. Naritomi et al. [13] speculated that ethanol may oxidize into acetate or pyruvate and be metabolized in the TCA cycle. In this study, the TCA cycle in the presence of ethanol was activated during the BC biosynthesis process by inducing the expressions of succinyl CoA synthetase, aconitate hydratase, succinate dehydrogenase and 3-oxoacyl-ACP synthase. The TCA cycle is the main energy production pathway involved in the biosynthesis of cellulose [12]. Succinyl CoA synthetase catalyzes inorganic phosphate molecules and nucleoside diphosphate molecules to form GTP or ATP [34], catalyzing key energy-generating reactions in the TCA cycle. Aconitate hydratase catalyzes the stereospecific isomerization of citrate into isocitrate via cis-aconitate, playing a role as an electron carrier in the TCA cycle [35]. Succinate dehydrogenase is the only enzyme that participates in both the TCA cycle and electron transport chain, which binds to the inner mitochondrial membranes and creates an electrochemical proton gradient that drives ATP synthesis in many types of bacterial cells [36]. Moreover, 3-Oxoacyl-ACP synthase is a transferase involved in the second reductive step of fatty acid biosynthesis [37], which is tangentially related to the TCA cycle [38]. These results provide powerful evidence to support Naritomi's speculation that ethanol can transform into acetic acid and flux into the TCA cycle [13]. However, Ryngajłło et al. [9] obtained a contrary conclusion that the presence of ethanol can inhibit the expression of the genes encoding enzymes in the TCA cycle. This discrepancy may be due to the difference of the species or strains used, since *K. xylinus* E25 was employed in that study.

Cellular energy is provided by mitochondria in the form of ATP through oxidative phosphorylation, of which the final step is catalyzed by transmembrane ATP synthase (FoF1-ATP synthase). Interestingly, in this study, three subunits (alpha, beta and gamma) of FoF1-ATP synthase were over-expressed during BC synthesis. Ethanol has been reported as an alternative energy source for ATP synthesis in *Komagataeibacter* [13], which can improve BC yield by promoting oxidative metabolism and the production of ATP, and provide enough energy for the TCA cycle [11]. The up-regulation of FoF1-ATP synthase subunits in this study provided direct evidence supporting this hypothesis. Generally, the ATP synthesis complex can utilize proton motive force and the corresponding membrane potential to synthesize ATP [39]. In the FoF1-ATP complex, the ATP synthase subunits alpha and beta are driven by protons flowing down an established electrochemical gradient. Then, ATP synthase subunits gamma acts as a rotary motor, helping ATP synthase subunits alpha and beta cross the inner membrane [40]. Meanwhile, the efficient expression of ATP synthase contributes to the rapid synthesis of BC. Moreover, inorganic pyrophosphatase

(*ppa*), a key kinase in oxidative phosphorylation, was up-regulated in *K. nataicola* Y19 during BC synthesis, which may facilitate the rapid circulation of energy consumption and replenishment.

To our knowledge, this study is the first report that links highly efficient BC production to chaperone DnaK, elongation factor Tu and preprotein translocase subunit SecB. The elongation factor Tu is a component of electron transfer complexes [41], as well as the regulator for the initial selection and subsequent proofreading of aa-tRNA [42]. The up-regulation of elongation factor Tu could promote the GTP–aa-tRNA complex to deliver aa-tRNA to the A-site of ribosomes [42]. Chaperone DnaK plays an essential role in protein folding and assembling, and newly synthesized polypeptide transportation [43]. In this research, the activation of elongation factor Tu and chaperone DnaK kept the stability of protein synthesis, which may guarantee the efficient synthesis of proteins in *K. nataicola* Y19 during BC production. Preprotein translocase subunit SecB interacts with the preprotein-conducing channel of SecYEG, which plays a central role in the hydrolysis of ATP and protein transformation through the cell membrane. SecYEG serves both as a receptor for the preprotein-SecB complex and as an ATP-driven molecular motor, driving the stepwise translocation of polypeptide chains to cross the membrane [44]. Higher expression of preprotein translocase subunit SecB may play a key role in the energy production in *K. nataicola* Y19.

On the other hand, further analysis revealed that endoglucanase in *K. nataicola* Y19 could be inhibited by the activation of BC biosynthesis in the presence of ethanol. Generally, endoglucanase could randomly cleave the cellulose β-1,4 linkages at internal amorphous sites [45]. However, in Kawano's research [27], the over-expression of the endoglucanase gene (*cmcax*) could enhance BC production in *A. xylinum*, which contrasted to our research. All these results indicate that the BC synthesis could be associated with the expression efficiency and activity of endoglucanase in *Komagataeibacter* spp. Assuredly, the effect of endoglucanase activity on BC synthesis is an interesting topic that should be further investigated in the future.

A network view demonstrating how ethanol regulates BC yield in bioprocesses by *K. nataicola* Y19 has been proposed (Figure 6).

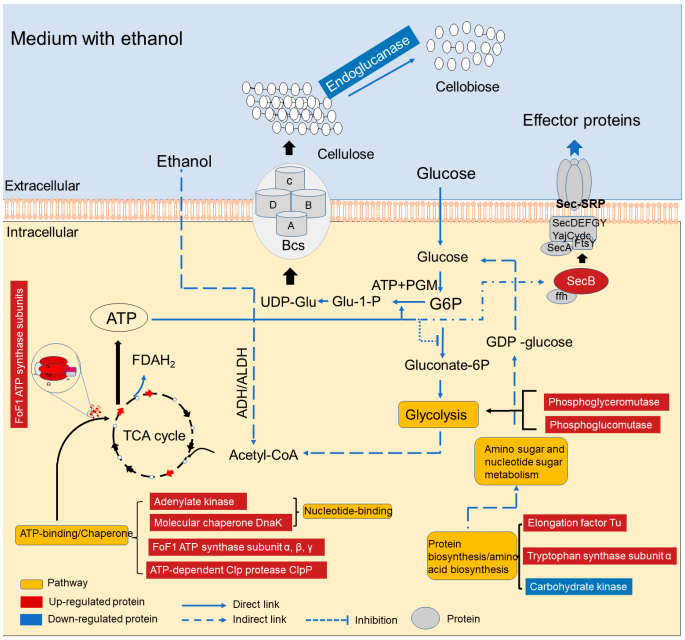

Figure 6. The metabolic pathway to bacterial cellulose biosynthesis in *K. nataicola* Y19 in the presence of ethanol. G6P: glucose-6-phosphate; Glu-1-P: glucose-1-phosphate; UDP-Glu: UDP-glucose; PGM: phosphoglucomutase; ADH: alcohol dehydrogenase; ALDH: acetaldehyde dehydrogenase. A-D: four subunits (BcsA, BcsB, BcsC and BcsD) of bacterial cellulose synthase (Bcs).

5. Conclusions

The present work presents a comparative proteomics analysis of *K. nataicola* Y19 after the addition of ethanol. The results showed that succinyl-CoA synthetase subunit alpha, aconitate hydratase, succinate dehydrogenase and 3-oxoacyl-ACP synthase in the TCA cycle were up-regulated, while phosphoglucomutase at the early stage of glycolysis was positively regulated. Additionally, FoF1-ATP synthase subunits (α, β and γ), elongation factor Tu and secretion chaperones DnaK and SecB were over-expressed. According to the results, the addition of ethanol may reduce the glucose consumption of *K. nataicola* Y19 by promoting its glucose phosphate translocation reaction during an early stage. *K. nataicola* Y19 could guarantee energy demand by promoting the oxidative phosphorylation and expression efficiency of ATPase. During BC production, the stability and efficiency of protein synthesis and cellulose secretion were maintained. Moreover, the results showed that endoglucanase expression was down-regulated, suggesting a potential correlation with the high BC yield. Further work is required to determine whether SecB and endoglucanase are directly associated with BC production. This study identified multiple key enzyme reaction sites related to the regulation of high BC production, providing a theoretical basis and valuable reference for research on BC synthetics biology, along with the yield improvement of nata de coco and their stable production in both the food industry and biomaterial industry.

Supplementary Materials: The following supporting information can be downloaded at: https://www.mdpi.com/article/10.3390/fermentation9060575/s1, Figure S1: Nata de coco pellicle of *K. nataicola* Y19 in media based on coconut water and coconut water with 1% ethanol for 7 d fermentation; Figure S2: Microfibril structure of the BC membrane of K.nataicola Y19 in the basal medium (CK) and the basal medium with ethanol and acetic acid; Figure S3: 2D gel profiles of total proteins of *K. nataicola* Y19 performed in triplicate.

Author Contributions: S.F.: Conceptualization, Formal analysis, Writing—original draft, Writing—review and editing. X.Y.: Conceptualization, Methodology, Investigation, Visualization, Writing—original draft. W.X.: Methodology. J.L. and H.C.: Visualization, Investigation. J.Z.: Software, Validation. X.L.: Data curation. S.L.: Conceptualization, Resources, Formal analysis, Funding acquisition, Writing—review and editing. C.L.: Funding acquisition, Supervision, Project administration. All authors have read and agreed to the published version of the manuscript.

Funding: This research was funded by the National Natural Science Foundation of China (No. 32060529, 31660458) and Key Research and Development Project of Hainan Province (No. ZDYF2020102).

Institutional Review Board Statement: Not applicable.

Informed Consent Statement: Not applicable.

Data Availability Statement: Data available on request from the authors.

Conflicts of Interest: The authors declare no conflict of interest.

Abbreviations

2D gels: two-dimensional gel; 3-oxoacyl-ACP synthase: 3-oxoacyl-ACP (acyl carrier protein) synthase; ATP: adenosine triphosphate; BC: bacterial cellulose; CAN: acetonitrile; CHAPS: 3-cholamidopropyl dimethylammonio 1-propanesulfonate; CHCA: α-cyano-4-hydroxy-cinnamic acid; DTT: dithiothreitol; EMP: Embden–Meyerhof–Parnas pathway; GDP: guanosine diphosphate. HMP: hexose mono-phosphate; HS: Hestrin–Schramm; IEF: isoelectric focusing; K. nataicola: Komagataeibacter nataicola; MALDI-TOF/TOF-MS: mass spectrometry MALDI ion source time-of-flight (TOF) mass; MLSA: multilocus sequence analysis; NCBI: National Center for Biotechnology Information; RT-qPCR: quantitative real-time PCR; SDS-PAGE: sodium dodecyl sulfate polyacrylamide gel electrophoresis; TCA cycle: tricarboxylic acid cycle; TFA: trifluoroacetic acid; UDP: uridine diphosphate glucose.

References

1. Ullah, H.; Santos, H.A.; Khan, T. Applications of bacterial cellulose in food, cosmetics and drug delivery. *Cellulose* **2016**, *23*, 2291–2314. [CrossRef]
2. Feng, Y.; Yin, N.; Zhou, Z.; Han, Y. Physical and antibacterial properties of bacterial cellulose films supplemented with cell-free supernatant enterocin-producing *Enterococcus faecium* TJUQ1. *Food Microbiol.* **2021**, *99*, 103828. [CrossRef]
3. Liu, X.; Xu, Y.; Guo, C.; Zhang, C.; Liu, S.; Gao, J.; Lin, G.; Yang, H.; Xia, W. Effect of chitosan grafting oxidized bacterial cellulose on dispersion stability and modulability of biodegradable films. *Int. J. Biol. Macromol.* **2022**, *204*, 510–519. [CrossRef]
4. Papadaki, A.; Manikas, A.C.; Papazoglou, E.; Kachrimanidou, V.; Lappa, I.; Galiotis, C.; Mandala, I.; Kopsahelis, N. Whey protein films reinforced with bacterial cellulose nanowhiskers: Improving edible film properties via a circular economy approach. *Food Chem.* **2022**, *385*, 132604. [CrossRef]
5. Fijałkowski, K.; Peitler, D.; Rakoczy, R.; Zywicka, A. Survival of probiotic lactic acid bacteria immobilized in different forms of bacterial cellulose in simulated gastric juices and bile salt solution. *LWT-Food Sci. Technol.* **2016**, *68*, 322–328. [CrossRef]
6. Li, Z.; Wang, X.; Wang, J.; Yuan, X.; Jiang, X.; Wang, Y.; Zhong, C.; Xu, D.; Gu, T.; Wang, F. Bacterial biofilms as platforms engineered for diverse applications. *Biotechnol. Adv.* **2022**, *57*, 107932. [CrossRef] [PubMed]
7. Andriani, D.; Apriyana, A.Y.; Karina, M. The optimization of bacterial cellulose production and its applications: A review. *Cellulose* **2020**, *27*, 6747–6766. [CrossRef]
8. Molina-Ramírez, C.; Enciso, C.; Torres-Taborda, M.; Zuluaga, R.; Gañán, P.; Rojas, O.J.; Castro, C. Effects of alternative energy sources on bacterial cellulose characteristics produced by *Komagataeibacter medellinensis*. *Int. J. Biol. Macromol.* **2018**, *117*, 735–741. [CrossRef]
9. Ryngajłło, M.; Jacek, P.; Cielecka, I.; Kalinowska, H.; Bielecki, S. Effect of ethanol supplementation on the transcriptional landscape of bionanocellulose producer *Komagataeibacter xylinus* E25. *Appl. Microbiol. Biotechnol.* **2019**, *103*, 6673–6688. [CrossRef]
10. Wang, S.-S.; Han, Y.-H.; Chen, J.-L.; Zhang, D.-C.; Shi, X.-X.; Ye, Y.-X.; Chen, D.-L.; Li, M. Insights into bacterial cellulose biosynthesis from different carbon sources and the associated biochemical transformation pathways in *Komagataeibacter* sp. W1. *Polymers* **2018**, *10*, 963. [CrossRef] [PubMed]
11. Abidi, W.; Torres-Sánchez, L.; Siroy, A.; Krasteva, P.V. Weaving of bacterial cellulose by the Bcs secretion systems. *FEMS Microbiol. Rev.* **2021**, *46*, fuab051. [CrossRef] [PubMed]
12. Li, G.; Wang, L.; Deng, Y.; Wei, Q. Research progress of the biosynthetic strains and pathways of bacterial cellulose. *J. Ind. Microbiol. Biotechnol.* **2022**, *49*, kuab071. [CrossRef] [PubMed]
13. Naritomi, T.; Kouda, T.; Yano, H.; Yoshinaga, F. Effect of ethanol on bacterial cellulose production from fructose in continuous culture. *J. Ferment. Bioeng.* **1998**, *85*, 598–603. [CrossRef]
14. Yunoki, S.; Osada, Y.; Kono, H.; Takai, M. Role of ethanol in improvement of bacterial cellulose production: Analysis using 13C-labeled carbon sources. *Food Sci. Technol. Res.* **2007**, *10*, 307–313. [CrossRef]
15. Sakurai, K.; Arai, H.; Ishii, M.; Igarashi, Y. Changes in the gene expression profile of Acetobacter aceti during growth on ethanol. *J. Biosci. Bioeng.* **2012**, *113*, 343–348. [CrossRef]
16. Hu, L.; Grim, C.J.; Franco, A.A.; Jarvis, K.G.; Sathyamoorthy, V.; Kothary, M.H.; McCardell, B.A.; Tall, B.D. Analysis of the cellulose synthase operon genes, bcsA, bcsB, and bcsC in Cronobacter species: Prevalence among species and their roles in biofilm formation and cell–cell aggregation. *Food Microbiol.* **2015**, *52*, 97–105. [CrossRef]
17. Jin, K.; Jin, C.; Wu, Y. Synthetic biology-powered microbial co-culture strategy and application of bacterial cellulose-based composite materials. *Carbohydr. Polym.* **2022**, *283*, 119171. [CrossRef]
18. Chien, L.J.; Chen, H.T.; Yang, P.F.; Lee, C.K. Enhancement of cellulose pellicle production by constitutively expressing Vitreoscilla hemoglobin in *Acetobacter xylinum*. *Biotechnol. Progr.* **2006**, *22*, 1598–1603. [CrossRef]
19. Liu, M.; Li, S.; Xie, Y.; Jia, S.; Hou, Y.; Zou, Y.; Zhong, C. Enhanced bacterial cellulose production by *Gluconacetobacter xylinus* via expression of Vitreoscilla hemoglobin and oxygen tension regulation. *Appl. Microbiol. Biotechnol.* **2018**, *102*, 1155–1165. [CrossRef]
20. Navarrete-Perea, J.; Gygi, S.P.; Paulo, J.A. Growth media selection alters the proteome profiles of three model microorganisms. *J. Proteomics* **2021**, *231*, 104006. [CrossRef] [PubMed]
21. Andrés-Barrao, C.; Saad, M.M.; Ferrete, E.C.; Bravo, D.; Chappuis, M.-L.; Pérez, R.O.; Junier, P.; Perret, X.; Barja, F. Metaproteomics and ultrastructure characterization of *Komagataeibacter* spp. involved in high-acid spirit vinegar production. *Food Microbiol.* **2016**, *55*, 112–122. [PubMed]
22. Román-Camacho, J.J.; Mauricio, J.C.; Santos-Dueñas, I.M.; García-Martínez, T.; García-García, I. Functional metaproteomic analysis of alcohol vinegar microbiota during an acetification process: A quantitative proteomic approach. *Food Microbiol.* **2021**, *98*, 103799. [CrossRef] [PubMed]
23. Lu, Z.; Zhang, Y.; Chi, Y.; Xu, N.; Yao, W.; Sun, B. Effects of alcohols on bacterial cellulose production by *Acetobacter xylinum* 186. *World J. Microbiol. Biotechnol.* **2011**, *27*, 2281–2285. [CrossRef]
24. Cheng, H.-T.; Hsieh, S.-Y.; Sung, C.-M.; Pai, B.C.-J.; Liu, N.-J.; Chen, C.P.C. Optimizing human bile preparation for Two-Dimensional gel electrophoresis. *Biomed. Res. Int.* **2016**, *2016*, 5185317. [CrossRef]
25. Sun, W.; Xing, B.; Sun, Y.; Du, X.; Lu, M.; Hao, C.; Lu, Z.; Mi, W.; Wu, S.; Wei, H. Proteome analysis of hepatocellular carcinoma by two-dimensional difference gel electrophoresis: Novel protein markers in hepatocellular carcinoma tissues. *Mol. Cell. Proteom.* **2007**, *6*, 1798–1808. [CrossRef]

26. Galisa, P.S.; da Silva, H.A.; Macedo, A.V.; Reis, V.M.; Vidal, M.S.; Baldani, J.I.; Simões-Araújo, J.L. Identification and validation of reference genes to study the gene expression in *Gluconacetobacter diazotrophicus* grown in different carbon sources using RT-qPCR. *J. Microbiol. Methods* **2012**, *91*, 1–7. [CrossRef]
27. Kawano, S.; Tajima, K.; Kono, H.; Numata, Y.; Yamashita, H.; Satoh, Y.; Munekata, M. Regulation of endoglucanase gene (cmcax) expression in *Acetobacter xylinum*. *J. Biosci. Bioeng.* **2008**, *106*, 88–94. [CrossRef]
28. Livak, K.J.; Schmittgen, T.D. Analysis of relative gene expression data using real-time quantitative PCR and the $2^{-\Delta\Delta CT}$ method. *Methods* **2001**, *25*, 402–408. [CrossRef]
29. Rachtanapun, P.; Jantrawut, P.; Klunklin, W.; Jantanasakulwong, K.; Gimeno, A.B. Carboxymethyl Bacterial Cellulose from Nata de Coco: Effects of NaOH. *Polymers* **2021**, *13*, 348. [CrossRef]
30. Kornmann, H.; Duboc, P.; Niederberger, P.; Marison, I.; Von Stockar, U. Influence of residual ethanol concentration on the growth of *Gluconacetobacter xylinus* I 2281. *Appl. Microbiol. Biotechnol.* **2003**, *62*, 168–173. [CrossRef] [PubMed]
31. Thakur, K.; Kumar, V.; Kumar, V.; Yadav, S.K. Genomic characterization provides genetic evidence for bacterial cellulose synthesis by *Acetobacter pasteurianus* RSV-4 strain. *Int. J. Biol. Macromol.* **2020**, 156. [CrossRef] [PubMed]
32. Jung, J.Y.; Khan, T.; Park, J.K.; Chang, H.N. Production of bacterial cellulose by *Gluconacetobacter hansenii* using a novel bioreactor equipped with a spin filter. *Korean J. Chem. Eng.* **2007**, *24*, 265–271. [CrossRef]
33. Li, Y.; Tian, C.; Tian, H.; Zhang, J.; He, X.; Ping, W.; Lei, H. Improvement of bacterial cellulose production by manipulating the metabolic pathways in which ethanol and sodium citrate involved. *Appl. Microbiol. Biotechnol.* **2012**, *96*, 1479–1487. [CrossRef]
34. Birney, M.; Um, H.-D.; Klein, C. Novel mechanisms of *Escherichia coli* succinyl-coenzyme A synthetase regulation. *J. Bacteriol.* **1996**, *178*, 2883–2889. [CrossRef]
35. Gardner, P.R. Aconitase: Sensitive target and measure of superoxide. In *Methods in Enzymology*; Academic Press: Cambridge, MA, USA, 2002; Volume 349, pp. 9–23.
36. Sun, L.; Zhou, F.; Shao, Y.; Lv, Z.; Li, C. The iron–sulfur protein subunit of succinate dehydrogenase is critical in driving mitochondrial reactive oxygen species generation in *Apostichopus japonicus*. *Fish Shellfish. Immun.* **2020**, *102*, 350–360. [CrossRef]
37. Gao, T.; Qian, S.; Shen, S.; Zhang, X.; Liu, J.; Jia, W.; Chen, Z.; Ye, J. Reduction of mitochondrial 3-oxoacyl-ACP synthase (OXSM) by hyperglycemia is associated with deficiency of α-lipoic acid synthetic pathway in kidney of diabetic mice. *Biochem. Biophys. Res. Commun.* **2019**, *512*, 106–111. [CrossRef] [PubMed]
38. Wickramasinghe, S.R.; Inglis, K.A.; Urch, J.E.; Müller, S.; Van Aalten, D.M.F.; Fairlamb, A.H. Kinetic, inhibition and structural studies on 3-oxoacyl-ACP reductase from *Plasmodium falciparum*, a key enzyme in fatty acid biosynthesis. *Biochem. J.* **2006**, *393*, 447–457. [CrossRef] [PubMed]
39. Taniguchi, N.; Suzuki, T.; Berney, M.; Yoshida, M.; Cook, G.M. Physiological importance of the ε subunit of bacterial FoF1-ATP synthase. *BBA-Bioenergetics* **2012**, *1817*, S25–S26. [CrossRef]
40. Watanabe, R.; Tabata, K.V.; Iino, R.; Noji, H. Direct observation of the rotation of FoF1-ATP synthase driven by the proton motive force. *BBA-Bioenergetics* **2012**, *1817*, S26–S27. [CrossRef]
41. Terasaki, M.; Suzuki, T.; Hanada, T.; Watanabe, K. Functional compatibility of elongation factors between mammalian mitochondrial and bacterial ribosomes: Characterization of GTPase activity and translation elongation by hybrid ribosomes bearing heterologous L7/12 proteins. *J. Mol. Biol.* **2004**, *336*, 331–342. [CrossRef]
42. Girodat, D.; Blanchard, S.C.; Wieden, H.J.; Sanbonmatsu, K.Y. Elongation Factor-Tu switch I is a gate for aminoacyl-tRNA selection. *J. Mol. Biol.* **2020**, *432*, 3064–3077. [CrossRef]
43. Hartl, F.U.; Hayer-Hartl, M. Converging concepts of protein folding in vitro and in vivo. *Nat. Struct. Mol. Biol.* **2009**, *16*, 574–581. [CrossRef] [PubMed]
44. de Cock, H.; Overeem, W.; Tommassen, J. Biogenesis of outer membrane protein PhoE of Escherichia coli: Evidence for multiple SecB-binding sites in the mature portion of the PhoE protein. *J. Mol. Biol.* **1992**, *224*, 369–379. [CrossRef] [PubMed]
45. Han, X.; Bi, R.; Khatri, V.; Oguzlu, H.; Takada, M.; Jiang, J.; Jiang, F.; Bao, J.; Saddler, J.N. Use of endoglucanase and accessory enzymes to facilitate mechanical pulp nanofibrillation. *ACS Sustain. Chem. Eng.* **2021**, *9*, 1406–1413. [CrossRef]